Retinoic Acid Upregulates Preadipocyte Genes to Block Adipogenesis and Suppress Diet-Induced Obesity

Daniel C. Berry,[1,2] David DeSantis,[2] Hooman Soltanian,[3] Colleen M. Croniger,[2] and Noa Noy[1,2]

Retinoic acid (RA) protects mice from diet-induced obesity. The activity is mediated in part through activation of the nuclear receptors RA receptors (RARs) and peroxisome proliferator–activated receptor β/δ and their associated binding proteins cellular RA binding protein type II (CRABP-II) and fatty acid binding protein type 5 in adipocytes and skeletal muscle, leading to enhanced lipid oxidation and energy dissipation. It was also reported that RA inhibits differentiation of cultured preadipocytes. However, whether the hormone suppresses adipogenesis in vivo and how the activity is propagated remained unknown. In this study, we show that RA inhibits adipocyte differentiation by activating the CRABP-II/RARγ path in preadipose cells, thereby upregulating the expression of the adipogenesis inhibitors Pref-1, Sox9, and Kruppel-like factor 2 (KLF2). In turn, KLF2 induces the expression of CRABP-II and RARγ, further potentiating inhibition of adipocyte differentiation by RA. The data also indicate that RA suppresses adipogenesis in vivo and that the activity significantly contributes to the ability of the hormone to counteract diet-induced obesity. ***Diabetes*** **61:1112–1121, 2012**

Obesity stems from hypertrophy of pre-existing adipocytes, resulting from excess lipid accumulation, and generation of new adipocytes through adipogenesis. Detailed understanding of the molecular mechanisms that regulate adipogenesis is thus important in the quest for strategies to overcome obesity and its associated pathologies. Current knowledge on these mechanisms is primarily based on investigations using cultured cell models, such as 3T3-L1 fibroblasts, that can be induced to differentiate into adipocytes upon treatment with a mixture of insulin, a glucocorticoid receptor agonist, and a phosphodiesterase inhibitor, which elevates adenosine 3′,5-cyclic monophosphate levels (1,2). These signaling molecules alter the expression of numerous genes, thereby triggering differentiation and allowing adipogenesis to proceed (3,4, reviewed in Ref. 5). In contrast, other signaling molecules negatively regulate adipocyte differentiation. One such important molecule is the vitamin A metabolite retinoic acid (RA). It has long been known that this hormone potently blocks adipogenesis when introduced at early stages of differentiation (6–8). It was subsequently reported that the loss of the inhibitory activity of RA at late stages stems from downregulation of the RA-activated transcription factor RA receptor (RAR) following induction of differentiation (9). It was also suggested that interference with adipogenesis by RA involves Smad3 (9–11). However, how RA regulates the expression of Smad3 is unknown, and, to date, the identity of genes that mediate RA-induced inhibition of adipocyte differentiation and the mechanisms by which the activity is propagated remained elusive.

RA regulates gene transcription by activating several members of the nuclear receptor family of ligand-activated transcription factors, the classical RARs—RARα, RARβ, and RARγ (12)—and the peroxisome proliferator–activated receptor β/δ (PPARβ/δ) (13–17). The partitioning of the hormone between its receptors is regulated by two intracellular lipid-binding proteins, cellular RA binding protein type II (CRABP-II), which delivers RA to RAR, and fatty acid binding protein type 5 (FABP5), which shuttles it to PPARβ/δ (15,16,18–22). We previously showed that adipocyte differentiation is accompanied by downregulation of RAR and CRABP-II and upregulation of PPARβ/δ and FABP5. Consequently, whereas in preadipocytes RA functions predominantly through CRABP-II and RAR, the hormone signals through both pathways in the mature adipocyte (13,14). Multiple studies established that RA treatment results in weight loss and enhances insulin sensitivity in various mouse models of obesity (13,23). These effects can be traced, at least in part, to enhanced fatty acid oxidation and energy dissipation brought about by RA-induced activation of PPARβ/δ and RAR in mature adipocytes, liver, and skeletal muscle (13,24).

Although the mechanisms by which RA regulates energy homeostasis and lipid metabolism in mature adipocytes are well understood, little information is available on functions of the hormone in preadipose cells. The hallmark of preadipocytes is Pref-1, a plasma membrane protein exclusively expressed in these cells that potently inhibits adipogenesis (25–27). Pref-1 is cleaved by a disintegrin and metalloprotease 17/tumor necrosis factor-α–converting enzyme to produce an extracellular active form that triggers extracellular signal-regulated kinase signaling, leading to induction of the transcription factor SOX9. In turn, SOX9 blocks adipogenesis by repressing the expression of the adipogenic factors CCAAT/enhancer binding protein (C/EBP) β and C/EBPδ (28–31). In accordance with inhibition of adipogenesis by the protein, it was reported that a low level of Pref-1 is associated with obesity in humans (32). Another protein that contributes to maintenance of the preadipocyte state is the transcription factor Kruppel-like factor 2 (KLF2), which inhibits adipogenesis by suppressing the expression of PPARγ, C/EBPα, and sterol regulatory element–binding protein 1c (SREBP1c) (33,34). The factors that control the expression of KLF2 or Pref-1 and its downstream effector SOX9 in preadipocytes are unknown.

This study was undertaken in order to delineate the mechanisms by which RA inhibits adipocyte differentiation

From the [1]Department of Pharmacology, Case Western Reserve University School of Medicine, Cleveland, Ohio; the [2]Department of Nutrition, Case Western Reserve University School of Medicine, Cleveland, Ohio; and the [3]Department of Plastic Surgery, Case Medical Center, Cleveland, Ohio.
Corresponding author: Noa Noy, noa.noy@case.edu.
Received 20 November 2011 and accepted 17 January 2012.
DOI: 10.2337/db11-1620
This article contains Supplementary Data online at http://diabetes.diabetesjournals.org/lookup/suppl/doi:10.2337/db11-1620/-/DC1.

and to examine whether this activity contributes to the ability of the hormone to prevent diet-induced obesity.

RESEARCH DESIGN AND METHODS

Reagents. All-*trans*-retinoic acid (RA) was from Calbiochem. Antibodies against Pref-1, Sox9, KLF2, and RARγ were from Santa Cruz Biotechnology. FABP4 antibodies were from R&D Systems. Pref-1 antibodies used in immunoblots were from Cell Signaling Technology. Lentiviruses harboring short hairpin RNAs (shRNAs) were from Open Biosystems. The triglyceride assay kit was from Zen-Bio.

Cells. Preadipocytes were cultured in Dulbecco's modified Eagle's medium (DMEM) supplemented with 10% calf serum. Two days postconfluence, cells were induced to differentiate in medium supplemented with 10% fetal bovine serum, 10 μg/mL insulin, 0.5 mmol/L 3-isobutyl-1-methylxanthine, and 0.25 mmol/L dexamethasone. NIH3T3-L1 cells were used unless otherwise specified. Experiments using preadipocytes were carried out at 70–80% confluency.

Quantitative real-time PCR. RNA was extracted and cDNA generated as described (13). TaqMan chemistry and assays on demand probes (Applied Biosystems) were: Pref-1, Mm00494477_m1, Hs00171584_m1; Sox9, Mm00448840, Hs00165814_m1; KLF2, Mm01244979_g1, Hs00360439_g1; C/EBPα, Mm00514283_s1; C/EBPβ, Mm00843434_s1; Adiponectin, Mm01343606_m1; FABP4, Mm00445880_m1; PPARγ, Mm01184322_m1; RARα, Mm043626_m; RARγ, Mm00441083_m1; CRABP-II, Mm00801691_m1; PPARβ/δ, Mm00803184; FABP5, Mm00783731_s1; and GAPDH, Mm99999915_g1.

Chromatin immunoprecipitation (ChIP) assays were carried out as described (13). PCR was performed using the following primer sets: RAR response element (RARE) Pref-1 sense, 5′-cttttcgtggtggttttcgt-3′ and antisense, 5′-gcaagtctcaggaaccaagc-3′; RARE Sox9 sense, 5′-agagcttcgccctcttagg-3′ and antisense, 5′-gttctgcttcttgcgtcctg-3′; RARE KLF2 sense, 5′-cctcttgctttctcca gagc-3′ and antisense, 5′-gtgcagggaagagctgttgt-3′; KLF2 site RARγ sense, 5′-cc ttattggtggccatggta-3′ and antisense, 5′-gacttgggttgcttggtgat-3′; and KLF2 site CRABP-II sense, 5′-tcaccgcactttcagctcta-3′ and antisense, 5′-gaggctagaag ggcagaggt-3′.

Isolation of human and mouse preadipocytes. Human adipose tissues were collected from patients undergoing abdominoplasty. Mouse preadipocytes were isolated from epididymal and inguinal fat depots. Preadipocytes were isolated as described (35) and passaged three times prior to experimentation.

Adipocyte differentiation. Preadipocytes were grown in DMEM supplemented with 10% calf serum. Differentiation media (DMEM supplemented with 10% fetal bovine serum, 10 μg/mL insulin [Sigma-Aldrich], 0.5 mmol/L 3-isobutyl-1-methylxanthine [Sigma-Aldrich], and 0.25 mmol/L dexamethasone [ThermoFisher]) was added 2 days past confluence. Three days later, medium was replaced with DMEM supplemented with 10% FBS for an additional 4 days.

Flow cytometry. Stromal-vascular (preadipocyte) and mature adipocyte fractions were isolated as described (35) and pooled. Pooled cells were stained with Nile red (50 μg/mL) and Hoechst dye 33342 (10 μmol/L) for 1 h in the dark. Cells were analyzed by flow cytometry (at 530 and 430 nm) to assess the fraction of Nile red-positive (lipid-containing) cells within total the Hoechst-positive cells.

Mice. Mouse studies were performed by the Mouse Metabolic Phenotyping Center of the Case Western Reserve University. All experiments used male mice. Lean mice were fed chow diet (LabDiet 5P76 Irradiated Isopro RMH 3000; Prolab, St. Louis, MO). Eight-week-old C57BL/6Ntac mice (Taconic Farms) mice were subcutaneously implanted with an RA pellet or mock pelleted by using a 10-gauge precision trochar (Innovative Research of America). Eight-week-old mice were placed on a high-fat/high-sucrose diet (HFHS; research diet D12331) as indicated. At the end of the experimental duration, mice were killed and tissues harvested following an overnight fast.

Body weights and food intake. Twenty-four–hour food consumption was measured once a week. During each 24-h period, mice were housed individually with a thin layer of bedding, and a known quantity of diet was provided. Food remaining after 24 h was weighed. Body weights were measured before and after the 24-h feeding period.

Blood parameters. Following an overnight fast, mice were killed and blood collected by a heart puncture. Plasma was isolated by using Microtainer plasma separator tubes (BD Biosciences). Leptin levels were measured using a leptin (mouse/rat) ELISA kit (ALPCO). Other parameters were measured by Veterinary Diagnostic Services (Marshfield Laboratories, Marshfield, WI).

Histology. Tissues were preserved in 10% formalin and then processed and sectioned by the Case Western Reserve University Histology Core. Sections were analyzed by using a Zeiss camera (Carl Zeiss).

Statistical Analyses. Data were analyzed by Student paired *t* test.

RESULTS

RA prevents diet-induced weight gain in mice. Eight-week-old C57BL/6Ntac male mice were used to examine effects of RA on dietary-induced obesity. Mice were fed an HFHS diet (research diet D12331). Animals in the experimental group were systemically treated by subcutaneous implantation of slow-release pellets (7.5 mg, 60-day release; Innovative Research of America). Preliminary results showed that this supraphysiological dose was effective but not toxic to the mice. Mice treated with RA were resistant to diet-induced weight gain despite a higher food intake as compared with control animals (Fig. 1*A* and *B*). The weight of white adipose tissue (WAT; combined epididymal and inguinal fat) of RA-treated mice was markedly lower as compared with WAT of nontreated animals (Fig. 1*C*), and histological examination showed that adipocyes in RA-treated mice were markedly smaller than in control animals (Fig. 1*D* and Supplementary Fig. 1*A*). RA treatment blunted diet-induced elevation in levels of plasma cholesterol (Fig. 1*E*) and plasma triglycerides (Fig. 1*F*) but did not affect levels of plasma free fatty acids (Fig. 1*G*).

RA treatment upregulated adipose PPARβ/δ target genes (e.g., 3-phosphoinositide-dependent protein kinase 1), which is involved in insulin signaling, and adipose differentiation-related protein, which is associated with lipid droplets. In addition, RA induced the expression of genes involved in regulating energy homeostasis that are under control of both RAR and PPARβ/δ, including uncoupling protein (UCP) 3, which mediates energy dissipation, and hormone-sensitive lipase (HSL), which catalyzes lipid hydrolysis (Fig. 1*H*). The data indicate that the ability of RA to protect animals from diet-induced obesity and insulin resistance is mediated, at least in part, by increasing the expression of adipose proteins that enhance lipid oxidation and energy dissipation and that promote insulin signaling.

To examine whether RA inhibits adipogenesis in vivo, adipose cells were isolated from WAT of control and RA-treated mice. Cells were stained with Hoechst stain and with the fluorescent lipid dye Nile red and analyzed by flow cytometry to assess the number of mature, lipid-accumulating cells in the tissues. The data (Fig. 1*I*) indicate that RA treatment decreased the content of mature adipocytes in WAT. Concomitantly, RA upregulated the expression of the preadipocyte marker Pref-1 in total adipose tissue (Fig. 1*J* and Supplementary Fig. 1*B*) and in the adipose stromal vascular fraction (Fig. 1*K*). Hence, the data indicate that RA treatment both upregulated the expression level of Pref-1 in cells that express this protein and increased the number of Pref-1–expressing cells. RA thus seem to contribute to maintenance of preadipocytes and inhibits adipocyte differentiation in vivo.

RARγ directly induces the expression of genes that inhibit adipogenesis. To investigate the mechanism by which RA inhibits adipocyte differentiation, the well-established cultured cell model of preadipocytes, NIH-3T3-L1 cells, and the pluripotent mesenchymal stem cell line C3H10T1/2 were used. Differentiation was induced by a standard protocol (see RESEARCH DESIGN AND METHODS) and monitored by examining the appearance of the adipocyte marker FABP4. Including RA in differentiation mixtures markedly inhibited adipogenesis both in NIH3T3-L1 and in C3H10T1/2 cells (Fig. 2*A* and Supplementary Fig. 5*A*). In agreement with the reports that RA functions in preadipocytes primarily through the CRABP-II/RAR pathway (13,14), the hormone did not inhibit differentiation in the presence of the pan-RAR antagonist LE540 (Fig. 2*A*). All of the components of the CRABP-II/RAR pathway in preadipocytes (i.e., CRABP-II, RARα, and RARγ) are downregulated following

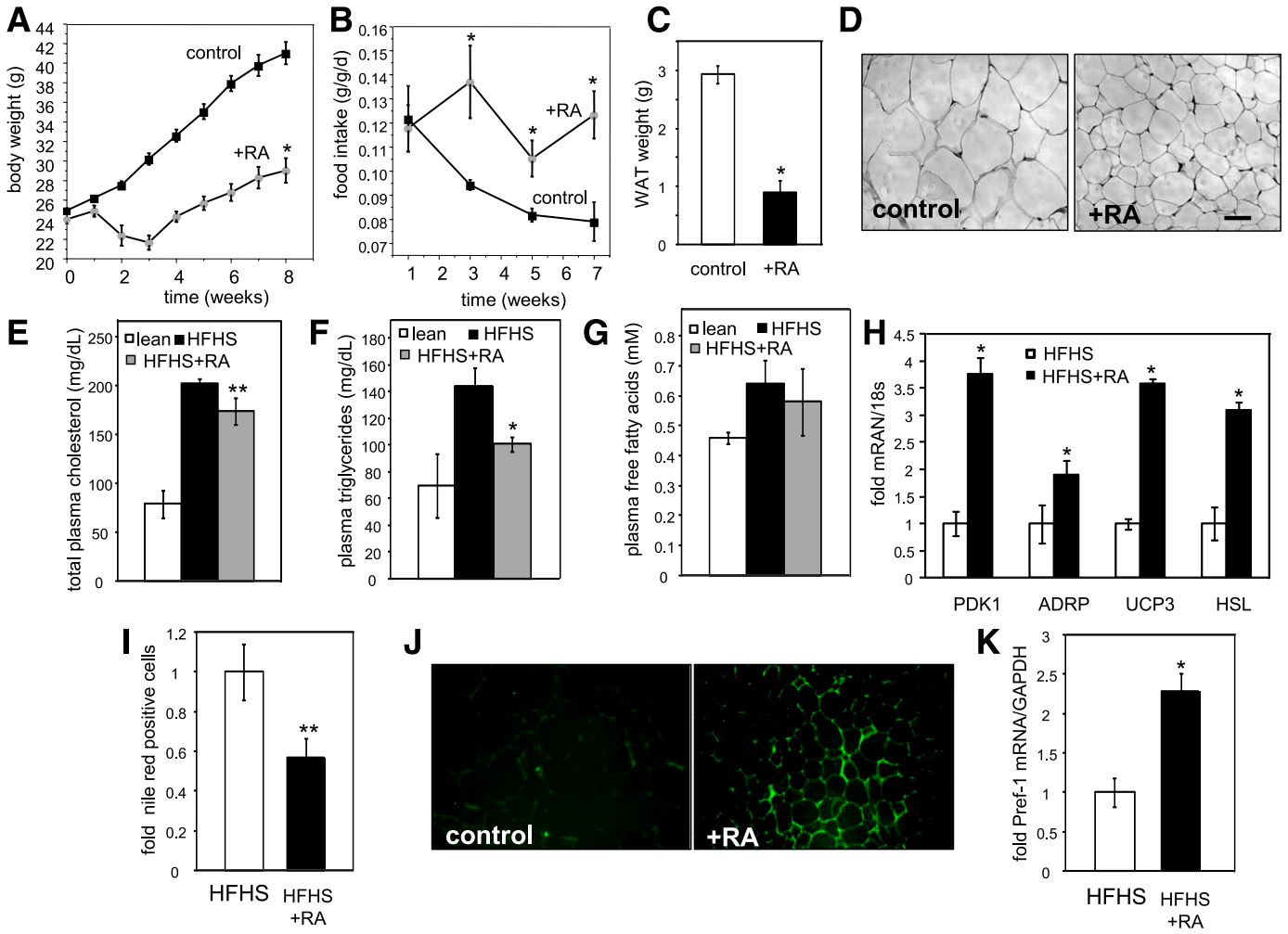

FIG. 1. RA prevents weight gain and inhibits adipogenesis in vivo. *A*: Body weight of control (black squares) and RA-treated (gray circles) 8-week-old mice fed an HFHS diet (n = 6/group) for 8 weeks. *B*: Food intake of control (black squares) and RA-treated (gray circles), normalized to body weight (n = 6/group). *C*: Weights of WAT in control and RA-treated mice (n = 3/group). *D*: Hematoxylin-eosin staining of adipose tissue of control and RA-treated mice. Plasma levels of total cholesterol (*E*), triglycerides (*F*), and free fatty acids (*G*) in lean mice (white bars), mice fed an HFHS diet for 8 weeks (black bars), and HFHS-fed RA-treated mice (HFHS+RA, gray bars). *H*: Levels of mRNA for denoted genes in WAT of untreated, HFHS-fed (white bars) and HSHF-fed, RA-treated mice (black bars). *I*: Cells were isolated from WAT of denoted mice, stained with Hoechst dye and Nile red, and analyzed by flow cytometry. Total of 10,000 cells was analyzed, and the fraction of Nile red-positive cells is shown. *J*: Pref-1 expression in WAT was visualized by immunofluorescence. *K*: Stromal vascular fraction was isolated from WAT and Pref-1 mRNA measured by quantitative real-time PCR (Q-PCR). Data are means ± SEM. n = 3/group unless denoted otherwise. *$P \le 0.01$; **$P \le 0.03$ HFHS-fed mice in the absence versus presence of RA treatment. (A high-quality digital representation of this figure is available in the online issue.)

induction of differentiation, but loss of RARγ is more pronounced than that of RARα (Fig. 2*B*). Overexpression of RARγ suppressed differentiation and enhanced the ability of RA to inhibit the process (Fig. 2*C* and *E*). Conversely, decreasing the level of RARγ enhanced differentiation and abrogated inhibition by RA (Fig. 2*D* and *E*). The observations thus demonstrate that downregulation of this receptor is critical for allowing differentiation to proceed.

Several proteins have been reported to effectively inhibit adipocyte differentiation. Among these is Pref-1, a signaling protein for which the downstream effector, transcription factor Sox9, inhibits adipogenesis by suppressing the expression of the adipogenic factors C/EBPβ and C/EBPδ (30,31,36,37). Another protein that was reported to inhibit adipogenesis is the transcription factor KLF-2, which suppresses PPARγ, C/EBPα, and SREBP1c expression (33,34).

RA and the pan-RAR agonist (*E*)-4-[2-(5,6,7,8-tetrahydro-5,5,8,8-tetramethyl-2-naphthylenyl)-1-propenyl] benzoic acid (TTNPB) induced expression of Pref-1, Sox9, and KLF2 in NIH-3T3-L1 cells (Fig. 2*F–I* and Supplementary Fig. 1*C*), C3H10T1/2 cells (Supplementary Fig. 5*B*), and primary human preadipocytes (Fig. 2*J*). The three genes were also upregulated in adipose tissue of mice treated with TTNPB or RA in vivo (Fig. 2*K*). RA and TTNPB induced the expression of these genes both in the absence and presence of the protein synthesis inhibitor cycloheximide (Fig. 2*F–H*), and the effect was abolished upon pretreatment with the pan-RAR antagonist LE540 (Fig. 2*L* and Supplementary Fig. 1*D* and *E*). Hence, Pref-1, SOX9, and KLF2 are direct targets for RAR. Examination of their respective promoter regions using Nubiscan (http://www.nubiscan.unibas.ch/) revealed putative RAR response elements in all three genes. Specifically, *Pref-1*, *SOX9*, and *KLF2* harbor the putative RAREs GGGTCAgaAGCCCA, AGTCCAagtcaAGGGCC, and AGTCCAagtcaAGGGCC at 563, 1370, and 1300 bp upstream from the respective transcription start sites. ChIP analyses were carried out to identify the RAR isotype that regulates the expression of the genes. The data (Fig. 3*A*) indicated that RARγ, but not RARα, is associated with the RAREs in the

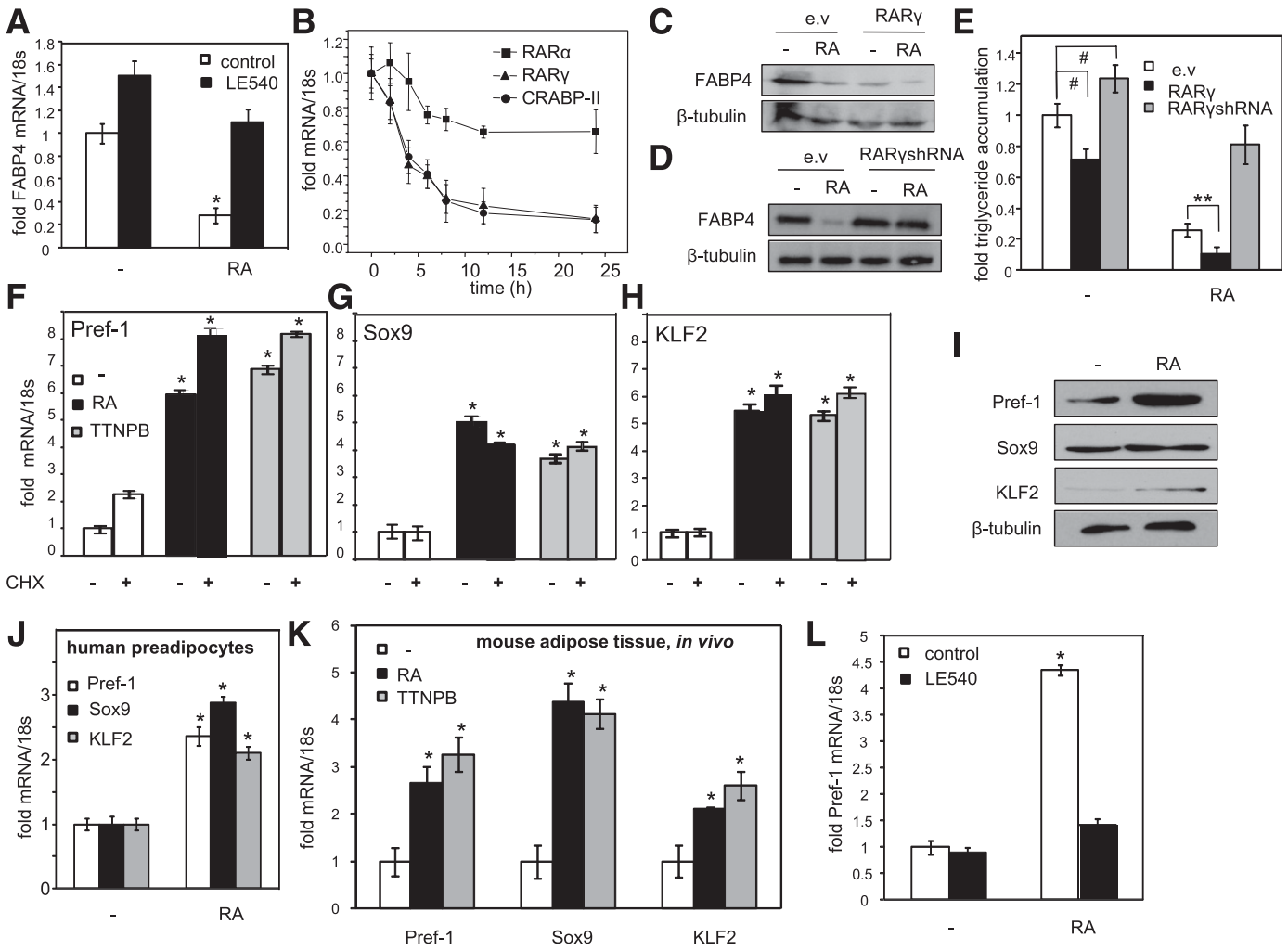

FIG. 2. RA induces the expression of the adipogenesis inhibitors Pref-1, Sox9, and KLF2. *A*: Levels of FABP4 mRNA in cells differentiated in the presence of RA, LE540, or both (1 μmol/L). **P* ≤ 0.01 control versus treated. *B*: Levels of RARα (■), RARγ (▲), and CRABP-II (●) mRNA of during the first 24 h of adipocyte differentiation. Preadipocytes were transfected with empty vector (e.v) or vector encoding RARγ (*C*) or infected with lentivirus encoding RARγ-shRNA (*D*) and then induced to differentiate in the absence or presence of RA (1 μmol/L). FABP4 expression was assessed by immunoblots. *E*: Triglyceride content of adipocytes treated as in *C* and *D*. #*P* ≤ 0.03 cells expressing e.v versus vector harboring RARγ or lentivirus encoding RARγ-shRNA; ***P* < 0.01 cells treated with RA expressing e.v versus vector harboring RARγ. *F*–*H*: Levels of denoted mRNAs in preadipocytes pretreated with cycloheximide (CHX; 15 min, 20 μg/mL) and then treated with vehicle (white bars), RA (black bars), or TTNPB (gray bars) (0.1 μmol/L, 4 h). **P* ≤ 0.01 control versus treated cells. *I*: Preadipocytes were treated with vehicle or RA (1 μmol/L, 8 h) and levels of Pref-1, Sox9, and KLF2 assessed by immunoblots. *J*: Levels of denoted mRNAs in human preadipocytes treated with vehicle or RA (0.1 μmol/L, 4 h). **P* ≤ 0.01 control versus treated. *K*: Levels of denoted mRNAs in adipose tissue of 22-week-old obese mice orally fed with vehicle (sesame oil, white bars), RA (black bars), or TTNPB (gray bars) daily for 2 days (0.16 mg ligand/day). *n* = 3/group. **P* ≤ 0.01 control versus RA-treated. *L*: Preadipocytes were pretreated with LE540 (1 μmol/L, 1 h) and then treated with vehicle (white bars) or RA (black bars) (1 μmol/L, 4 h). Pref-1 mRNA was measured by Q-PCR. Data are means ± SD from three independent experiments.

Pref-1 and Sox9 promoters. It is worth noting that SOX9 was previously found to also comprise a direct target for RAR in breast cancer cells (38). Both RAR isotypes were found to be associated with the RARE of the KLF2 promoter, but binding of RARγ was stronger than that of RARα. The elements were also occupied by RXR, demonstrating the presence of a functional RAR-RXR heterodimer. It is worth noting that recruitment of the RAR-RXR heterodimers to the response element was independent of the presence of RA. To further examine the relative contributions of RARγ and RARα, their expression levels were modulated. Ectopic overexpression of RARγ, but not RARα, upregulated Pref-1 (Fig. 3*B*) and Sox9 (Supplementary Fig. 2*A*). KLF2 was induced by both RARs (Supplementary Fig. 2*B*). Critical involvement of RARγ was further demonstrated by the observation that decreasing the expression of this isotype abolished the RA response of all three genes (Fig. 3*C*). As expected from bona fide RAR targets, upregulation of Pref-1, SOX9, and KLF2 by RA was enhanced by ectopic expression of CRABP-II (Fig. 3*D* and Supplementary Fig. 2*D* and *E*).

RA potently induced the expression of Pref-1, SOX9, and KLF2 at early stages of adipocyte differentiation but was much less effective at later stages (Fig. 3*E*–*G*). These observations, likely reflecting the loss of CRABP-II and RARγ following differentiation induction (Fig. 2*B*), provide a rationale for understanding why RA is effective in inhibiting adipocyte differentiation only early in the process (9).

Inhibition of adipogenesis by RA is mediated by Pref-1 and Sox9. The expression of Pref-1 and Sox9 in preadipocytes was decreased using respective shRNAs (Supplementary

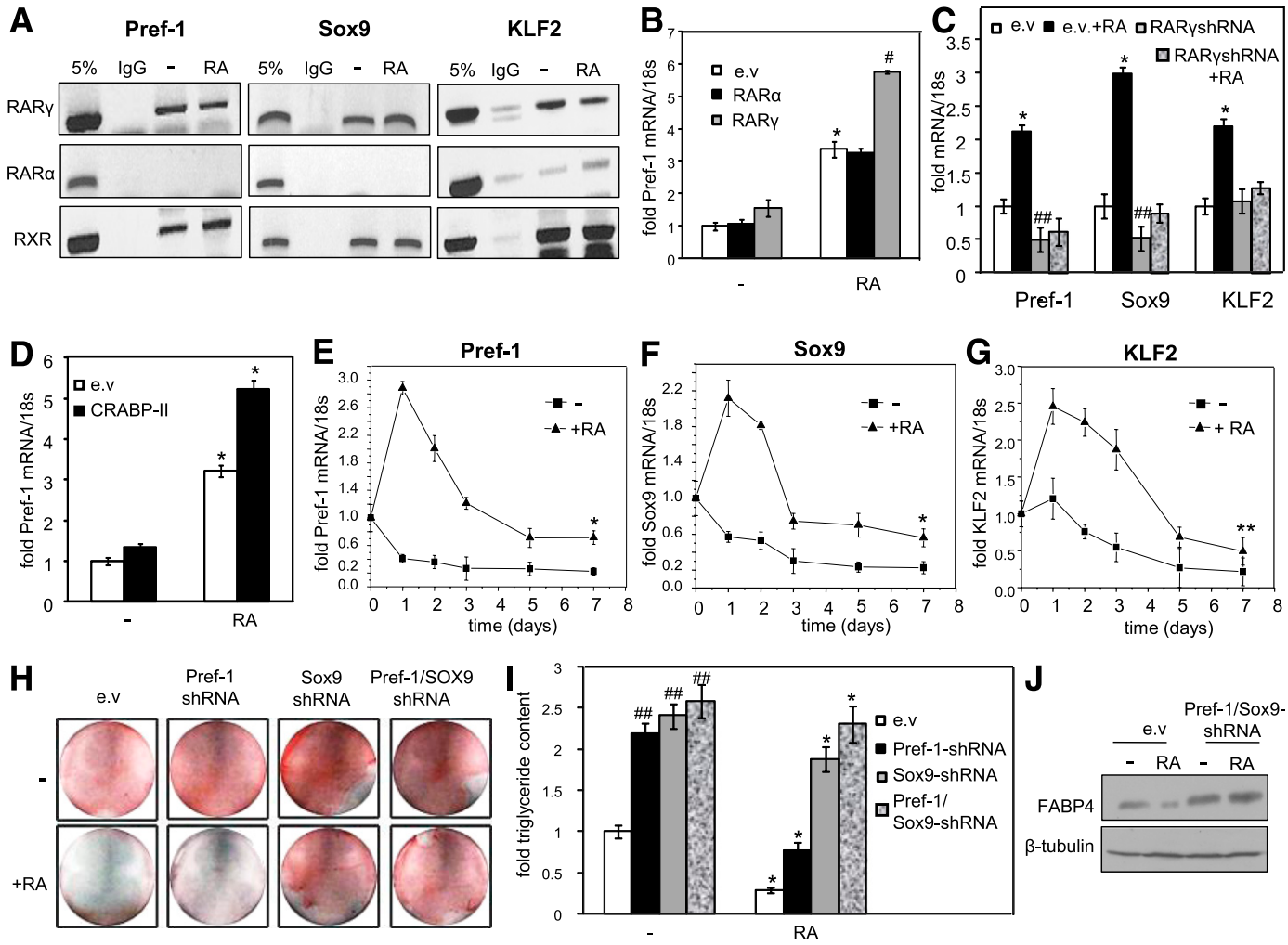

FIG. 3. Pref-1, Sox9, and KLF2 are direct RAR target genes and mediate RA-induced inhibition of adipogenesis. *A*: ChIP analysis of RAREs located in the promoters of denoted genes. Analyses were carried out using antibodies against denoted RARs. A pan-RXR antibody was used to examine the recruitment of this receptor. *B*: Preadipocytes were transfected with vectors encoding empty vector (e.v, white bars), RARα (black bars), or RARγ (gray bars) for 24 h. Overexpression was verified by immunoblots (Supplementary Fig. 2*C*). Cells were then treated with RA (0.1 μmol/L, 4 h). Pref-1 mRNA was measured by Q-PCR. **P* < 0.01 control versus RA-treated; #*P* < 0.01 RA-treated empty virus-expressing cells versus RA-treated RARγ-expressing cells. *C*: Preadipocytes were infected with lentivirus encoding RARγ-shRNA or empty virus. Reduced expression was verified by immunoblots (Supplementary Fig. 2*C*). Cells were then treated with RA (0.1 μmol/L, 4 h). Levels of denoted mRNAs were assessed by Q-PCR. **P* < 0.01 control versus RA-treated; ##*P* < 0.05 nontreated empty virus–expressing cells versus nontreated denoted shRNA-expressing cells. *D*: Preadipocytes were infected with empty adenovirus (e.v, white bars) or adenovirus encoding CRABP-II (black bars); 24 h later, cells were treated or not with RA (1 μmol/L, 4 h). Pref-1 mRNA was measured by Q-PCR. **P* < 0.01 control versus RA-treated cells. *E–G*: NIH-3T3-L1 cells were induced to differentiate, and levels of mRNAs for denoted genes were monitored throughout differentiation in the absence (■) or presence of RA (+RA, ▲) (1 μmol/L). RA was replenished every 2 days. **P* < 0.01 control versus RA-treated; ***P* < 0.05 control versus RA-treated. *H–J*: Preadipocytes stably expressing shRNA for Pref-1, Sox9, or both were induced to differentiate in the presence of RA (1 μmol/L). Adipocyte differentiation was monitored by Oil Red O staining (*H*), by measuring triglyceride content (*I*), and by immunoblotting FABP4 (*J*). **P* < 0.01 control versus RA-treated; ##*P* < 0.05 nontreated e.v-expressing cells versus nontreated cells expressing denoted shRNA. Data are means ± SD from three independent experiments.

Fig. 3*A*), and cells were then induced to differentiate in the presence or absence of RA. Differentiation was assessed by Oil Red O staining, measurements of the triglyceride content of cells, and monitoring the expression of various adipocyte markers. Downregulation of Sox9 or of both Sox9 and Pref-1 enhanced differentiation and abrogated the inhibitory activity of RA both in NIH3T3-L1 cells (Fig. 3*H–J* and Supplementary Fig. 3*B–D*) and C3H10T1/2 cells (Supplementary Fig. 5*C* and *D*). In contrast, reducing the expression of Pref-1 alone was not as effective (Fig. 3*H* and *I*). The latter observation can be readily understood considering that SOX9, the downstream effector of Pref-1, is itself a direct target for RAR. As SOX9 is induced by RA independently of Pref-1 (Supplementary Fig. 4*A* and *B*), RA can inhibit differentiation even in the absence of the latter.

Inhibition of adipogenesis by RA is mediated and enhanced by KLF2. To examine the involvement of KLF2 in RA-induced inhibition of adipogenesis, the factor was ectopically overexpressed in preadipocytes. Cells were then induced to differentiate in the presence of varying concentrations of RA. Ectopic expression of KLF2 effectively inhibited adipogenesis and markedly potentiated the inhibitory activity of RA (Fig. 4*A* and *B*). Conversely, decreasing the expression of KLF2 enhanced adipogenesis and abrogated the ability of RA to inhibit the differentiation of NIH3T3-L1 (Fig. 4*C–E*) and C3H10T1/2 cells (Supplementary Fig. 5*E* and *F*).

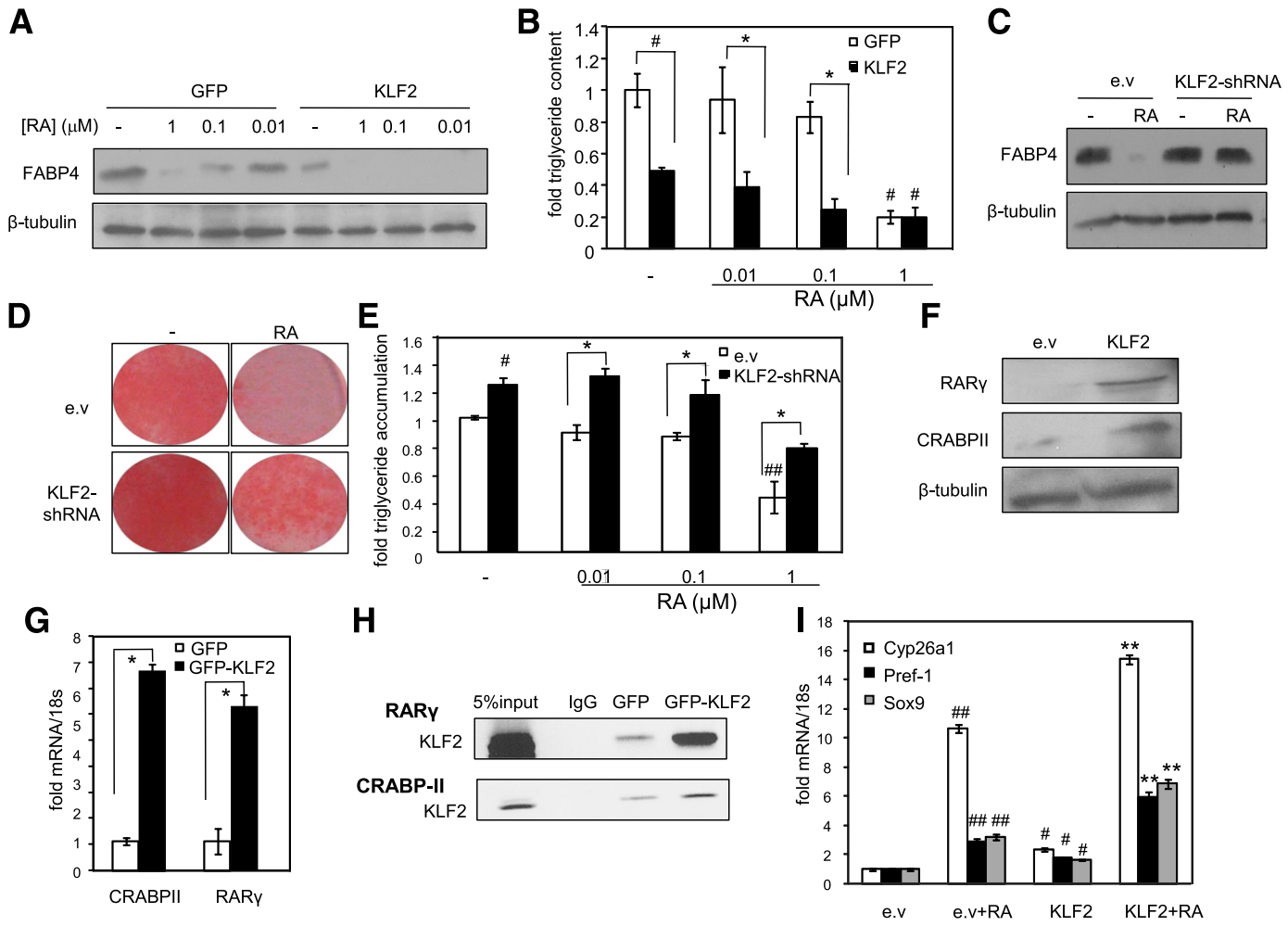

FIG. 4. RA inhibits adipogenesis through KLF2, which, in turn, feeds back onto RA signaling. *A*: Preadipocytes were infected with retroviruses encoding green fluorescent protein (GFP) or GFP-KLF2 and treated with denoted concentrations of RA throughout differentiation. RA was replenished every 48 h. FABP4 expression was monitored by immunoblots. *B*: Preadipocytes, infected with retroviruses encoding GFP (white bars) or GFP-KLF2 (black bars), were induced to differentiate in the presence of denoted concentrations of RA. Triglyceride content was measured. #$P \leq 0.01$ cells infected with GFP versus GFP-KLF2–encoding vector; *$P < 0.05$ RA-treated cells expressing GFP versus RA-treated GFP-KLF2–expressing cells. *C–E*: Preadipocytes were infected with an empty lentivirus (e.v, white bars) or lentivirus encoding KLF2-shRNA (black bars) and induced to differentiate in the absence or presence of RA (1 μmol/L). Differentiation was monitored by immunoblotting for FABP4 (*C*), Oil Red O staining (*D*), and measuring triglyceride content (*E*). #$P \leq 0.01$ cells infected with GFP versus GFP-KLF2–encoding vector; *$P < 0.05$ RA-treated cells expressing GFP versus RA-treated GFP-KLF2–expressing cells; ##$P < 0.001$ RA-treated versus nontreated cells. *F*: Preadipocytes were infected with retrovirus encoding KLF2. Expression levels of denoted proteins were analyzed by immunoblotting. *G*: Preadipocytes were infected with retroviruses encoding GFP (white bars) or GFP-KLF2 (black bars). Levels of mRNA for denoted genes were assessed by Q-PCR. *$P < 0.05$ RA-treated cells expressing GFP versus RA-treated GFP-KLF2–expressing cells. *H*: Preadipocytes were infected with retroviruses encoding GFP or GFP-KLF2. ChIP analyses were carried out using KLF2 antibodies. PCR was conducted to amplify the regions containing the KLF response element in the promoters of RARγ and CRABP-II. *I*: Preadipocytes were infected with a retrovirus encoding GFP or GFP-KLF2 and then treated with RA (0.1 μmol/L, 4 h). Levels of mRNA for Cyp26a1 (white bars), Pref-1 (black bars), and Sox9 (gray bars) were measured by Q-PCR. ##$P < 0.001$ RA-treated versus nontreated cells; #$P \leq 0.01$ cells infected with GFP versus GFP-KLF2–encoding vector; **$P < 0.001$ RA-treated cells expressing GFP versus RA-treated GFP-KLF2–expressing cells. Data are means ± SD from three separate experiments.

Interestingly, ectopic expression of KLF2 led to upregulation of CRABP-II and RARγ (Fig. 4*F* and *G*). Examination of the promoters of these genes revealed the presence of KLF2 response elements in both. Specifically, the RARγ gene harbors a 5′-CACCC-3′ sequence at +105 bp, and CRABP-II harbors three tandem KLF2 elements,, 5′-CACCCCCACCCCCACCACCC-3′, at −763 bp. ChIP assays demonstrated that KLF2 occupies these elements in preadipocytes (Fig. 4*H*). Hence, KLF2 is placed within a positive-feedback loop that promotes the transcriptional activities of RA through the CRABP-II/RARγ path. In accordance with this notion, overexpressing KLF2 enhanced the ability of RA to upregulate the expression of the hallmark RAR target gene Cyp26a1 as well as the newly identified RAR targets Pref-1 and Sox9 (Fig. 4*I*).

Decreasing RA signaling through the CRABP-II/RAR pathway promotes diet-induced adipogenesis and obesity in vivo. Inhibition of adipocyte differentiation by RA, exerted by activating the CRABP-II/RAR path, may contribute to the ability of the hormone to suppress diet-induced obesity. To examine this notion, 8-week-old CRABP-II heterozygous (C57/Bl6/CRABP-II$^{+/-}$) mice and wild-type (WT) littermates were used. The reduced expression of CRABP-II in these mice is expected to decrease the transcriptional activity of RAR. Expression levels of the adipocyte markers FABP4 and PPARγ in WT and CRABP-II$^{+/-}$ mice were similar, demonstrating that mature adipocytes in CRABP-II$^{+/-}$ mice retain normal phenotype (Supplementary Fig. 4*C*). In agreement with the identification of Pref-1, SOX9, and KLF2 as CRABP-II/RAR targets, the levels of

these genes were markedly lower in adipose tissue of CRABP-II$^{+/-}$ versus WT mice (Fig. 5*A*). The reduced expression of these adipocyte inhibitors suggests that CRABP-II$^{+/-}$ mice are prone to excess adipogenesis. If so, it may be predicted that high-fat feeding of these mice will result in enhanced adiposity. In accordance with this notion, CRABP-II$^{+/-}$ mice fed an HFHS diet gained more weight than WT animals (Fig. 5*B*), although they displayed lower food intake (Fig. 5*C*). The increased weight stemmed from a higher weight of WAT and liver (Fig. 5*D*). The observed hepatic steatosis (Fig. 5*E*) is in keeping with the report that RA enhances lipid oxidation and inhibits lipid biosynthesis in the liver of mice (39). Remarkably, the size of adipocytes in WT and CRABP-II$^{+/-}$ mice was similar (Fig. 5*F* and *G*). Hence, the increase in the weight of WAT in these animals did not result from enhanced hypertrophy but, instead, reflected accelerated generation of mature adipocytes. The levels of Pref-1, SOX9, and KLF2 in CRABP-II$^{+/-}$ mice remained lower than in WT animals following 13 weeks on a high-fat diet (Fig. 5*H*).

In mature adipocytes, RAR upregulates HSL and UCP1 (13,40) and represses the expression of leptin (41). Reflecting a reduced RAR activity in CRABP-II$^{+/-}$ mice, expression of adipose HSL and UCP1 was lower, and expression of leptin was higher in these animals (Fig. 6*A*). The resulting increased serum level of leptin (Fig. 6*A*, *inset*) provides a rationale for understanding the reduced food intake in these animals (Fig. 5*C*). In contrast with RAR target genes, the expression of adipose genes that are regulated by RA through activation of PPARβ/δ, including 3-phosphoinositide-dependent protein kinase 1, adipose differentiation-related protein, aldehyde dehydrogenase 9, and UCP3 (13), was similar in CRABP-II$^{+/-}$ and WT mice (Fig. 6*A*). Hence, the reduced expression of CRABP-II did not hamper the ability of RA to activate PPARβ/δ in mature adipocytes. CRABP-II$^{+/-}$ mice also displayed normal plasma levels of cholesterol, triglycerides, and free fatty acids, parameters that were previously shown to be controlled by RA through the FABP5/PPARβ/δ pathway (Fig. 6*B–D*).

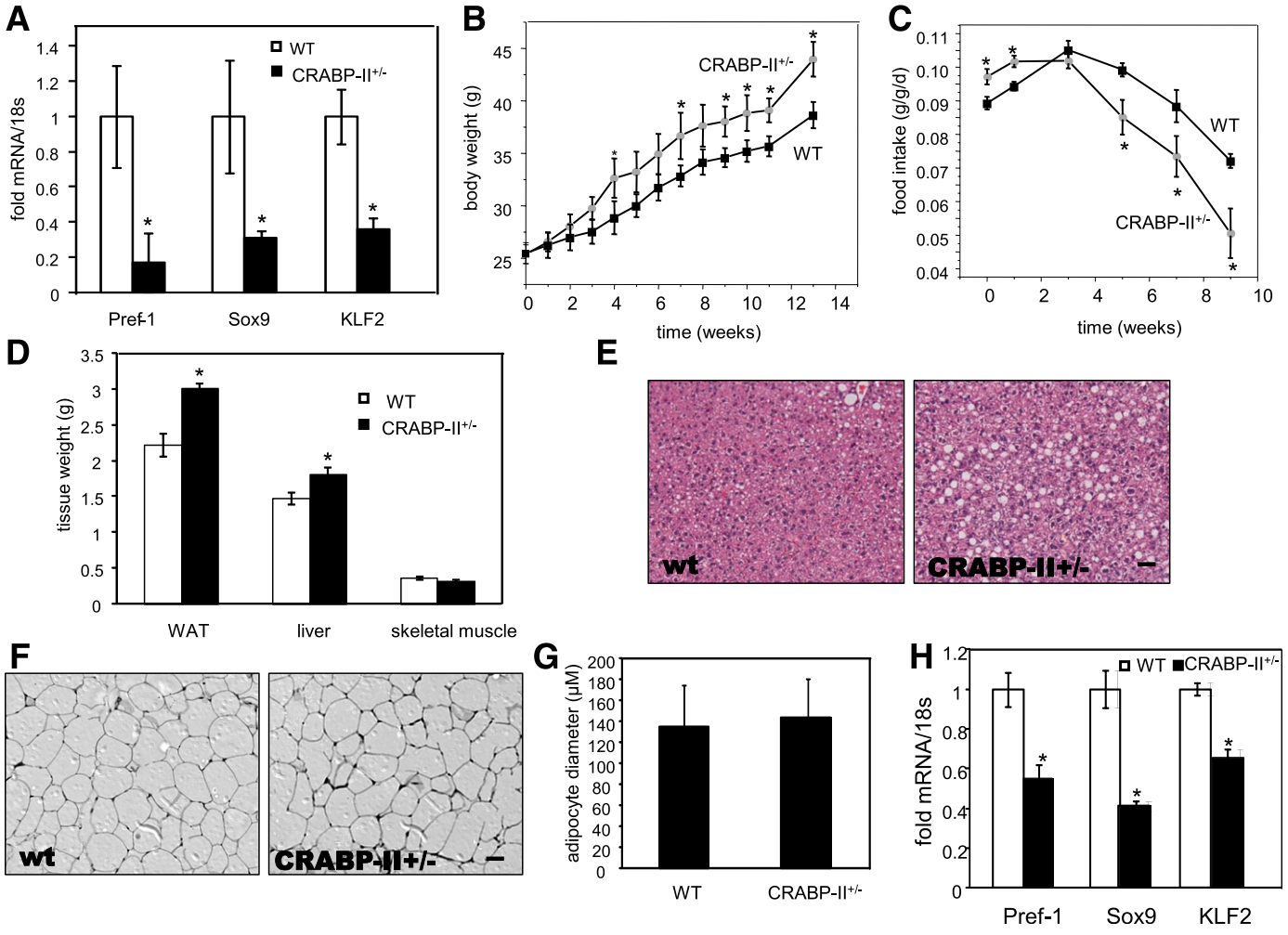

FIG. 5. Decreasing CRABP-II expression exacerbates obesity by promoting adipocyte differentiation in vivo. *A*: Levels of denoted mRNAs from WAT of WT (white bars) and CRABP$^{-/+}$ (black bars) mice fed a normal chow diet (n = 3). *B*: Body weight of 8-week-old WT (black squares) or CRABP-II$^{+/-}$ (gray circles) mice fed an HFHS diet (WT: n = 4; CRABP-II$^{+/-}$: n = 3). *C*: Food intake of WT (black squares) or CRABP-II$^{+/-}$ (gray circles) mice fed an HFHS diet, normalized to body weight (WT: n = 4; CRABPII$^{+/-}$: n = 3). *D*: Weights of WAT, liver, and skeletal muscle in WT (white bar) and CRABP$^{+/-}$ (gray bar) mice following 14 weeks of HFHS feeding. Hematoxylin-eosin staining of liver (*E*) and adipose tissue (*F*) of WT and CRABP-II$^{+/-}$ mice following 14 weeks of HFHS feeding. *G*: Adipocyte diameters in WT and CRABP-II$^{+/-}$ mice following 14 weeks of HFHS feeding. Total of 50 adipocytes per adipose tissue were measured (n = 3 mice/group). *H*: Levels of mRNAs for denoted genes in WAT of WT (white bar) and WAT of CRABP-II$^{+/-}$ (black bar) mice following 14 weeks of HFHS feeding (n = 3/group). Data are mean ± SEM. *P < 0.05 WT versus CRABP-II$^{+/-}$ mice. (A high-quality color representation of this figure is available in the online issue.)

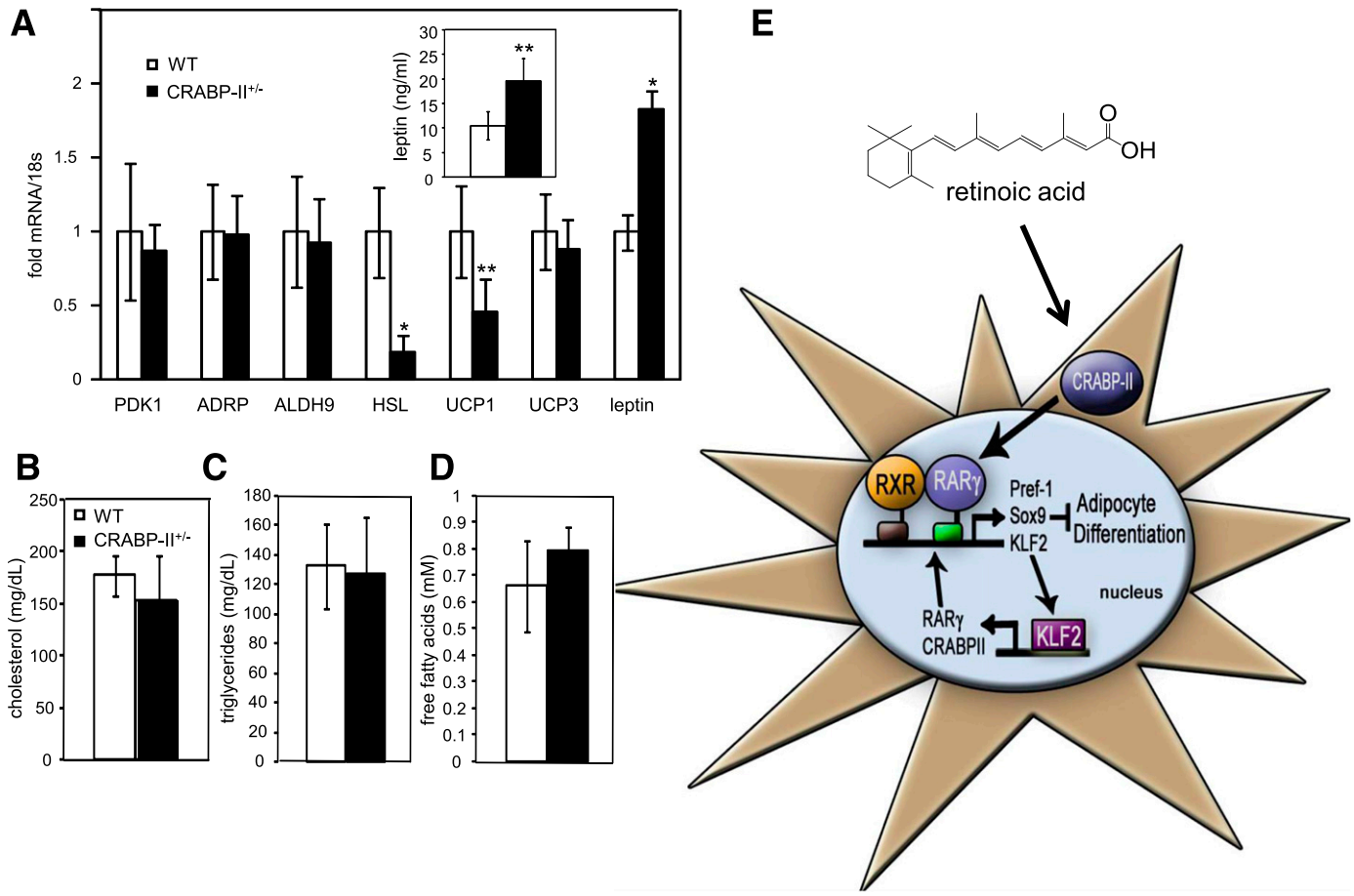

FIG. 6. Effect of decreasing CRABP-II expression on adipose genes and blood parameters. *A*: Levels of denoted mRNAs from WAT of WT (white bars) and CRABP-II$^{+/-}$ (black bars) mice (n = 3/group). *Inset*: serum levels of leptin in blood of WT and CRABP-II$^{+/-}$ mice following 14 weeks of HFHS feeding (n = 3 to 4/group). Plasma concentrations of cholesterol (*B*), triglycerides (*C*), and free fatty acids (*D*) in WT (white bars) and CRABP-II$^{+/-}$ (black bars) mice (n = 3 to 4/group). Data are means ± SEM. *E*: A model for RA-induced inhibition of adipogenesis. In preadipocytes, RA activates CRABP-II and RARγ to induce expression of Pref-1, Sox9, and KLF2, which, in turn, potently inhibit adipogenesis. KLF2 upregulates RARγ and CRABP-II, thereby propagating a positive-feedback loop that further potentiates RA induced inhibition of adipocyte differentiation. *P < 0.01; **P = 0.04 WT versus CRABP-II$^{+/-}$ mice.

DISCUSSION

Multiple reports demonstrated that the vitamin A metabolite RA induces weight lost and enhances insulin sensitivity in obese mice (13,23). In further support of the conclusion that RA plays an important role in regulating body weight, it was also reported that mice lacking retinol dehydrogenase 1, an enzyme that catalyzes the first step in the conversion of retinol to RA, display increased size and obesity (42). One mechanism by which RA induces weight loss involves activation of RAR and PPARβ/δ in adipocytes, liver, and skeletal muscle, resulting in upregulation of genes that promote lipolysis, lipid oxidation, energy dissipation, and insulin sensitivity (13,14) (Fig. 1*H*). RA thus prevents diet-induced weight gain and adipose hypertrophy (Fig. 1*A*–*D*) and protects mice from high-fat diet–induced elevation in serum levels of cholesterol and triglycerides (Fig. 1*E* and *F*). It is noteworthy that, whereas RA treatment lowered serum triglyceride levels in mice, it has been reported that administration of the agent to human patients leads to hypertriglyceridemia (43–46). The differential response may reflect species specificities. However, as biochemical abnormalities in human patients appear only at high RA doses (45,46), it is possible that hypertriglyceridemia may be avoided if RA is used at subtoxic doses. The efficacy of a low-dose RA treatment in overcoming obesity and insulin resistance in humans remains to be examined.

In addition to modulating lipid metabolism and energy utilization, RA suppresses the generation of new adipocytes in cultured cells and, as we show in this study, in vivo (Fig. 1*I*–*K*). The data demonstrate that this activity is mediated by CRABP-II cooperating mainly with the RAR isotype RARγ, albeit with some contribution of RARα (Fig. 3*A*–*D*). These RA-activated RARs inhibit adipogenesis through induction of target genes that encode the adipogenesis inhibitors Pref-1, Sox9, and KLF2 (Fig. 6*E*).

It was previously reported that inhibition of adipogenesis by RA originates from interference of RAR with the activity of the early adipogenic factor C/EBP-β and that the effect may be mediated by Smad3 (9–11). Our observations that RA induces the expression of Pref-1 suggest an alternative mechanism for inhibition of C/EBPs by RA. Pref-1 inhibits adipogenesis by triggering mitogen-activated protein kinase/extracellular signal-regulated kinase signaling, leading to upregulation of Sox9, which, in turn, suppresses the transcription of both C/EBP-β and C/EBP-δ (30,36). The data described in this study demonstrate that RARγ induces the expression of Pref-1 as well as SOX9, providing a direct rationale for understanding the inhibition of C/EBPs by RA. The involvement of Smad3 in the activity

remains to be clarified. Transgenic mice that overexpress Pref-1 in adipose tissue display partial lipodystrophy and, accordingly, hypertriglyceridemia (47). Notably, induction of Pref-1 by RA was not accompanied by biochemical abnormalities and did not lead to lipodystrophy. The data thus indicate that RA treatment of mice fed a high-fat diet moderated adipogenesis but did not completely block the process. Likely, induction of Pref-1 by RA increased the expression level of the protein to a lesser extent than that achieved by transgenic overexpression (47). Taken together with the report that a low level of Pref-1 is associated with obesity in humans (32), these observations support the notions that RA may be efficacious in treatment of obesity and that it does so in part by increasing the expression of Pref-1.

KLF2 inhibits adipocyte differentiation by suppressing the expression of PPARγ, C/EBPα, and SREBP1c (33,34). We show in this study that KLF2 is a direct RAR target in preadipocytes (Fig. 2*H*) and that, in turn, the factor induces the expression of RARγ and CRABP-II (Fig. 4*H*). KLF2 is thus placed within a positive-feedback loop that promotes RA signaling through CRABP-II and RARγ, thereby further enhancing inhibition of adipogenesis by the hormone (Fig. 6*E*). Interestingly, a similar cross-talk between KLF2 and RA signaling was recently found to occur in MCF-7 mammary carcinoma cells in which KLF2 functions as a tumor suppressor (48). In MCF-7 cells, RA promotes proliferation and survival when directed toward PPARβ/δ by FABP5 but inhibits growth when targeted to RAR by CRABP-II (15,49,50). The tumor-suppressive activities of KLF2 may thus be exerted through its ability to modulate RA signaling (48). The cross-talk between KLF2 and the RA machinery in cancer development remains to be investigated.

CRABP-II$^{+/-}$ mice fed an HFHS diet displayed increased adipose tissue mass (Fig. 5*D*) but a similar adipocyte size as compared with WT counterparts (Fig. 5*F*). These observations must reflect that the number of adipocytes is higher in the CRABP-II$^{+/-}$ mice. Hence, enhanced weight gain in CRABP-II$^{+/-}$ mice did not stem from adipocyte hypertrophy but originated directly from enhanced adipogenesis. These observations demonstrate that decreasing RA signaling through the CRABP-II/RAR pathway resulted in resistance to inhibition of adipogenesis by RA. Consequently, HFHS intake led to massive adipogenesis and enhanced adiposity in CRABP-II$^{+/-}$ mice. Taken together, these and previous observations demonstrate that RA regulates adipose tissue biology by two distinct activities: in preadipocytes, RA activates CRABP-II and RAR to inhibit adipocyte differentiation, and in mature adipocytes, RA activates both the CRABP-II/RAR and FABP5/PPARβ/δ paths to promote lipid oxidation and energy utilization. RA thus suppresses dietary-induced obesity by counteracting both adipogenesis and adipocyte hypertrophy.

ACKNOWLEDGMENTS

This work was supported by National Institutes of Health (NIH) Grant R01-DK-060684 to N.N. D.C.B. was supported in part by NIH Grant T3-DK-073195. The Mouse Metabolic Phenotyping Center of the Case Western Reserve University is supported by NIH Grant DK-59630.

No potential conflicts of interest relevant to this article were reported.

D.C.B. designed experiments, collected data, and wrote the article. D.D. collected data. H.S. provided human adipose tissue. C.M.C. provided advice and assisted in animal studies. N.N. formulated experiments, analyzed data, and cowrote the manuscript and is the guarantor of this work and, as such, had full access to all the data in the study and takes responsibility for the integrity of the data and the accuracy of the data analysis.

The authors thank Vincent Giguere (McGill University, Montreal, Quebec, Canada) for sharing CRABP-II$^{+/-}$ mice, Hiroyuki Kagechika (Tokyo Medical and Dental University, Tokyo, Japan) for providing the RAR antagonist LE-540, Cecile Rochette-Egly (Institut de Génétique et de Biologie Moléculaire et Cellulaire, Strasbourg, France) for CRABP-II antibodies, and Mukesh Jain (Case Western Reserve University, Cleveland, OH) for the KLF2 retrovirus.

REFERENCES

1. Green H, Kehinde O. An established preadipose cell line and its differentiation in culture. II. Factors affecting the adipose conversion. Cell 1975;5:19–27
2. Green H, Meuth M. An established pre-adipose cell line and its differentiation in culture. Cell 1974;3:127–133
3. Tontonoz P, Hu E, Graves RA, Budavari AI, Spiegelman BM. mPPAR gamma 2: tissue-specific regulator of an adipocyte enhancer. Genes Dev 1994;8:1224–1234
4. Shao D, Lazar MA. Peroxisome proliferator activated receptor gamma, CCAAT/enhancer-binding protein alpha, and cell cycle status regulate the commitment to adipocyte differentiation. J Biol Chem 1997;272:21473–21478
5. Farmer SR. Transcriptional control of adipocyte formation. Cell Metab 2006;4:263–273
6. Murray T, Russell TR. Inhibition of adipose conversion in 3T3-L2 cells by retinoic acid. J Supramol Struct 1980;14:255–266
7. Sato M, Hiragun A, Mitsui H. Preadipocytes possess cellular retinoid binding proteins and their differentiation is inhibited by retinoids. Biochem Biophys Res Commun 1980;95:1839–1845
8. Kuri-Harcuch W. Differentiation of 3T3-F442A cells into adipocytes is inhibited by retinoic acid. Differentiation 1982;23:164–169
9. Xue JC, Schwarz EJ, Chawla A, Lazar MA. Distinct stages in adipogenesis revealed by retinoid inhibition of differentiation after induction of PPARgamma. Mol Cell Biol 1996;16:1567–1575
10. Schwarz EJ, Reginato MJ, Shao D, Krakow SL, Lazar MA. Retinoic acid blocks adipogenesis by inhibiting C/EBPbeta-mediated transcription. Mol Cell Biol 1997;17:1552–1561
11. Marchildon F, St-Louis C, Akter R, Roodman V, Wiper-Bergeron NL. Transcription factor Smad3 is required for the inhibition of adipogenesis by retinoic acid. J Biol Chem 2010;285:13274–13284
12. Germain P, Chambon P, Eichele G, et al. International Union of Pharmacology. LX. Retinoic acid receptors. Pharmacol Rev 2006;58:712–725
13. Berry DC, Noy N. All-trans-retinoic acid represses obesity and insulin resistance by activating both peroxisome proliferation-activated receptor beta/delta and retinoic acid receptor. Mol Cell Biol 2009;29:3286–3296
14. Berry DC, Soltanian H, Noy N. Repression of cellular retinoic acid-binding protein II during adipocyte differentiation. J Biol Chem 2010;285:15324–15332
15. Schug TT, Berry DC, Shaw NS, Travis SN, Noy N. Opposing effects of retinoic acid on cell growth result from alternate activation of two different nuclear receptors. Cell 2007;129:723–733
16. Schug TT, Berry DC, Toshkov IA, Cheng L, Nikitin AY, Noy N. Overcoming retinoic acid-resistance of mammary carcinomas by diverting retinoic acid from PPARbeta/delta to RAR. Proc Natl Acad Sci USA 2008;105:7546–7551
17. Shaw N, Elholm M, Noy N. Retinoic acid is a high affinity selective ligand for the peroxisome proliferator-activated receptor beta/delta. J Biol Chem 2003;278:41589–41592
18. Dong D, Ruuska SE, Levinthal DJ, Noy N. Distinct roles for cellular retinoic acid-binding proteins I and II in regulating signaling by retinoic acid. J Biol Chem 1999;274:23695–23698
19. Budhu AS, Noy N. Direct channeling of retinoic acid between cellular retinoic acid-binding protein II and retinoic acid receptor sensitizes mammary carcinoma cells to retinoic acid-induced growth arrest. Mol Cell Biol 2002;22:2632–2641
20. Manor D, Shmidt EN, Budhu A, et al. Mammary carcinoma suppression by cellular retinoic acid binding protein-II. Cancer Res 2003;63:4426–4433

21. Sessler RJ, Noy N. A ligand-activated nuclear localization signal in cellular retinoic acid binding protein-II. Mol Cell 2005;18:343–353
22. Tan NS, Shaw NS, Vinckenbosch N, et al. Selective cooperation between fatty acid binding proteins and peroxisome proliferator-activated receptors in regulating transcription. Mol Cell Biol 2002;22:5114–5127
23. Bonet ML, Ribot J, Palou A. Lipid metabolism in mammalian tissues and its control by retinoic acid. Biochim Biophys Acta 2012;1821:177–189
24. Mercader J, Madsen L, Felipe F, Palou A, Kristiansen K, Bonet ML. All-trans retinoic acid increases oxidative metabolism in mature adipocytes. Cell Physiol Biochem 2007;20:1061–1072
25. Wang Y, Kim KA, Kim JH, Sul HS. Pref-1, a preadipocyte secreted factor that inhibits adipogenesis. J Nutr 2006;136:2953–2956
26. Moon YS, Smas CM, Lee K, et al. Mice lacking paternally expressed Pref-1/Dlk1 display growth retardation and accelerated adiposity. Mol Cell Biol 2002;22:5585–5592
27. Villena JA, Choi CS, Wang Y, et al. Resistance to high-fat diet-induced obesity but exacerbated insulin resistance in mice overexpressing preadipocyte factor-1 (Pref-1): a new model of partial lipodystrophy. Diabetes 2008;57:3258–3266
28. Smas CM, Chen L, Sul HS. Cleavage of membrane-associated pref-1 generates a soluble inhibitor of adipocyte differentiation. Mol Cell Biol 1997; 17:977–988
29. Wang Y, Sul HS. Ectodomain shedding of preadipocyte factor 1 (Pref-1) by tumor necrosis factor alpha converting enzyme (TACE) and inhibition of adipocyte differentiation. Mol Cell Biol 2006;26:5421–5435
30. Wang Y, Zhao L, Smas C, Sul HS. Pref-1 interacts with fibronectin to inhibit adipocyte differentiation. Mol Cell Biol 2010;30:3480–3492
31. Wang Y, Sul HS. Pref-1 regulates mesenchymal cell commitment and differentiation through Sox9. Cell Metab 2009;9:287–302
32. O'Connell J, Lynch L, Hogan A, Cawood TJ, O'Shea D. Preadipocyte factor-1 is associated with metabolic profile in severe obesity. J Clin Endocrinol Metab 2011;96:E680–E684
33. Banerjee SS, Feinberg MW, Watanabe M, et al. The Krüppel-like factor KLF2 inhibits peroxisome proliferator-activated receptor-gamma expression and adipogenesis. J Biol Chem 2003;278:2581–2584
34. Wu J, Srinivasan SV, Neumann JC, Lingrel JB. The KLF2 transcription factor does not affect the formation of preadipocytes but inhibits their differentiation into adipocytes. Biochemistry 2005;44:11098–11105
35. Bakker AH, Van Dielen FM, Greve JW, Adam JA, Buurman WA. Preadipocyte number in omental and subcutaneous adipose tissue of obese individuals. Obes Res 2004;12:488–498
36. Sul HS. Minireview: Pref-1: role in adipogenesis and mesenchymal cell fate. Mol Endocrinol 2009;23:1717–1725
37. Kim KA, Kim JH, Wang Y, Sul HS. Pref-1 (preadipocyte factor 1) activates the MEK/extracellular signal-regulated kinase pathway to inhibit adipocyte differentiation. Mol Cell Biol 2007;27:2294–2308
38. Afonja O, Raaka BM, Huang A, et al. RAR agonists stimulate SOX9 gene expression in breast cancer cell lines: evidence for a role in retinoid-mediated growth inhibition. Oncogene 2002;21:7850–7860
39. Amengual J, Ribot J, Bonet ML, Palou A. Retinoic acid treatment enhances lipid oxidation and inhibits lipid biosynthesis capacities in the liver of mice. Cell Physiol Biochem 2010;25:657–666
40. Rabelo R, Reyes C, Schifman A, Silva JE. A complex retinoic acid response element in the uncoupling protein gene defines a novel role for retinoids in thermogenesis. Endocrinology 1996;137:3488–3496
41. Felipe F, Mercader J, Ribot J, Palou A, Bonet ML. Effects of retinoic acid administration and dietary vitamin A supplementation on leptin expression in mice: lack of correlation with changes of adipose tissue mass and food intake. Biochim Biophys Acta 2005;1740:258–265
42. Zhang M, Hu P, Krois CR, Kane MA, Napoli JL. Altered vitamin A homeostasis and increased size and adiposity in the rdh1-null mouse. FASEB J 2007;21:2886–2896
43. Castaigne S, Chomienne C, Daniel MT, et al. All-trans retinoic acid as a differentiation therapy for acute promyelocytic leukemia. I. Clinical results. Blood 1990;76:1704–1709
44. Kanamaru A, Takemoto Y, Tanimoto M, et al.; Japan Adult Leukemia Study Group. All-trans retinoic acid for the treatment of newly diagnosed acute promyelocytic leukemia. Blood 1995;85:1202–1206
45. Conley BA, Egorin MJ, Sridhara R, et al. Phase I clinical trial of all-trans-retinoic acid with correlation of its pharmacokinetics and pharmacodynamics. Cancer Chemother Pharmacol 1997;39:291–299
46. Jones PH, Burnett RD, Fainaru I, et al. A phase 1 study of tazarotene in adults with advanced cancer. Br J Cancer 2003;89:808–815
47. Lee K, Villena JA, Moon YS, et al. Inhibition of adipogenesis and development of glucose intolerance by soluble preadipocyte factor-1 (Pref-1). J Clin Invest 2003;111:453–461
48. Kannan-Thulasiraman P, Seachrist DD, Mahabeleshwar GH, Jain MK, Noy N. Fatty acid-binding protein 5 and PPARbeta/delta are critical mediators of epidermal growth factor receptor-induced carcinoma cell growth. J Biol Chem 2010;285:19106–19115
49. Donato LJ, Noy N. Suppression of mammary carcinoma growth by retinoic acid: proapoptotic genes are targets for retinoic acid receptor and cellular retinoic acid-binding protein II signaling. Cancer Res 2005;65:8193–8199
50. Donato LJ, Suh JH, Noy N. Suppression of mammary carcinoma cell growth by retinoic acid: the cell cycle control gene Btg2 is a direct target for retinoic acid receptor signaling. Cancer Res 2007;67:609–615